

Dennes T. Bergado,¹ Hary C. Hardiyatimo,² Chilvier B. Cisneros,² Chai Jin Chun,³ Marolo C. Alfaro,⁴ A. S. Balasubramaniam,⁵ and Loren R. Anderson⁶

Pullout Resistance of Steel Geogrids with Weathered Clay as Backfill Material

REFERENCE: Bergado, D. T., Hardiyatimo, H. C., Cisneros, C. B., Chun, C. J., Alfaro, M. C., Balasubramaniam, A. S., and Anderson, L. R., "Pullout Resistance of Steel Geogrids with Weathered Clay as Backfill Material," *Geotechnical Testing Journal*, GTJODJ, Vol. 15, No. 1., March 1992, pp. 33-46.

ABSTRACT: The pullout resistance of welded steel geogrid reinforcement embedded in poor-quality, cohesive-frictional backfill material such as weathered clay was investigated. Laboratory pullout tests were conducted on various reinforcement sizes, mesh geometry, and compaction conditions of the backfill material. Field pullout tests were also conducted to investigate the pullout resistance of reinforcements embedded at representative overburden, field moisture, and density conditions. The soil-reinforcement interaction indicated the dominant role of passive or bearing resistance contributed by the transverse members to the total pullout resistance. The frictional resistance of the longitudinal members was found to contribute only about 5 to 15% of the total pullout resistance. It was observed that the reinforcement moved nearly as a rigid body and that the pullout resistance along the reinforcement is uniformly mobilized. The field pullout test provided higher pullout resistance compared to that of the laboratory test. Comparison of the predicted pullout bearing resistance with the observed data indicated that the prediction based on the bearing failure model formed the upper boundary while the prediction associated with the punching failure model provided the lower boundary. An empirical equation was proposed to predict the bearing resistance of the transverse members with reasonable accuracy.

KEY WORDS: reinforcement, soil, soil reinforcement, geogrid, pullout test, compaction, water content, earthfill

Owing to its flexible construction method and competitive cost, earth reinforcement techniques have gained enormous applicability to geotechnical engineering infrastructures such as retaining walls and embankments. A variety of reinforcements have

been employed, from steel strips and steel geogrids to polymer grids and geotextiles. However, the backfill materials commonly used consist of the ideal granular materials.

In the Chao Phraya Plain of Thailand in which the Bangkok metropolis is located, poor-quality, cohesive-frictional soils are abundant. High-quality granular soils are scarce and usually located far from construction sites and thus are expensive due to high transportation costs. On the other hand, the use of polymer materials as reinforcement becomes expensive due to high import tax. Consequently, it is imperative to utilize cheaper, locally available but poor-quality backfill materials in conjunction with steel geogrid reinforcements which can be fabricated locally. Several investigators (Ingold 1983; Jewell et al. 1984; Fabian 1987; Abdel-Motaleb 1989; Hannon and Forsyth 1984) have studied the interaction between the reinforcements and cohesive-frictional backfill materials. A full-scale welded steel geogrid reinforced wall/embankment system was constructed inside the Asian Institute of Technology (AIT) campus, located 42 km north of Bangkok, to investigate the behavior of mechanically stabilized earth (MSE) constructions with cohesive-frictional backfills on soft ground (Bergado et al. 1991). Field and laboratory pullout tests were conducted in conjunction with the above investigation to understand the interaction mechanisms between the welded steel geogrid reinforcement and cohesive-frictional backfill materials.

Engineering Properties of Compacted Weathered Bangkok Clay

The weathered Bangkok clay is the uppermost surface layer of about 2.0-m-thick dark-brown weathered clay crust overlying the soft Bangkok clay deposit. The index and basic properties are given in Table 1, while the grain-size distribution is shown in Fig. 1. The strength, deformation, and permeability characteristics of compacted weathered Bangkok clay have been studied by several researchers (Leelasithorn 1977; Haque 1977; Plangpongpon 1977; Liew 1978) in connection with the settlement and stability analyses of embankments. The strength parameters based on direct shear, unconsolidated-undrained (UU) and consolidated-undrained (CIU) triaxial tests were also investigated for the study of the interaction with welded steel geogrid reinforcement (Cisneros 1989; Hardiyatimo 1990). The relevant results from these studies are summarized in Table 2. The compression test results indicated that compacted weathered

¹Associate professor, Division of Geotechnical and Transportation Engineering (GTE), Asian Institute of Technology (AIT), G.P.O. Box 2754, Bangkok, 10501, Thailand.

²Former graduate student, GTE Division, AIT, G.P.O. Box 2754, Bangkok, Thailand.

³Doctoral student, GTE Division, AIT, G.P.O. Box 2754, Bangkok, Thailand.

⁴Research Associate, GTE Division, AIT, G.P.O. Box 2754, Bangkok, Thailand.

⁵Professor, GTE Division, AIT, G.P.O. Box 2754, Bangkok, Thailand.

⁶Professor, Department of Civil and Environmental Engineering, Utah State University, Logan, Utah 84322-4110.

TABLE 1—Index and basic properties of weathered Bangkok clay.

Soil Description	G _s	% Passing No. 200	Liquid Limit, %	Plastic Limit, %	Plasticity Index, %	$\gamma_{d_{max}}$, kN/m ³	w_{opt} , %
Dark brown weathered clay	2.67	83.25	45.0	21.0	24.0	16.0	23.3

GRAVEL		SAND			SILT	CLAY
Coarse	Fine	Coarse	Medium	Fine		
Percent 0.0	0.0	0.7	4.4	11.7	23.8	59.5

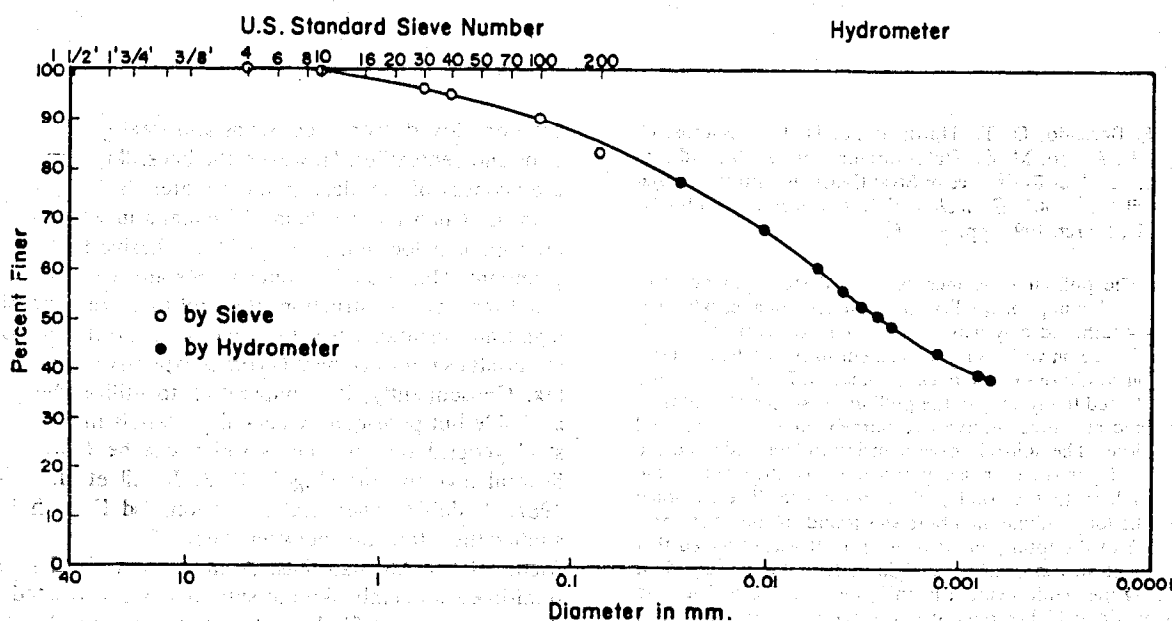


FIG. 1—Typical grain-size distribution of weathered Bangkok clay.

TABLE 2—Strength, deformation and permeability properties of compacted weathered Bangkok Clay.

Strength Properties								Compression Index	Permeability, cm/s	Swelling Index	Tension, kPa
Direct Shear		UU Triaxial		CIU Triaxial							
c, kPa	ϕ , deg.	c, kPa	ϕ , deg.	c, kPa	ϕ , deg.	c', kPa	ϕ' , deg.				
73.0 ^a	21.4 ^a	118.0	31.5	19.0	25.8	24.0	15.5	0.08–0.12	10 ⁻⁷	0.005–0.025	25.0–35.0
89.0 ^b	32.2 ^b										

^aCompacted at the wet side of optimum water content.^bCompacted at the dry side of optimum water content.

Bangkok clay behaved like a natural stiff clay with the coefficient of compressibility, C_c , ranging from 0.08 to 0.12 (Liew 1978). The swelling property is controlled by dry density and water content. Higher dry density and lower water content cause larger swelling and swell pressure. For dry densities within 14 to 16 kN/m³ and compaction water content between 23 and 27%, the free swelling index is in the range of 0.5 to 2.5%. The tension strength ranged between 25 to 35 kPa, corresponding to maximum density and compaction water content of 24 to 25% (Lee-lasithorn 1977). Two compaction water content conditions were investigated, namely, dry side and wet side of optimum. Dry side and wet side of optimum water contents are designated

herein as the water contents, with variation of $\pm 1\%$, corresponding to 95% of the maximum standard Proctor [ASTM Test Methods for Moisture-Density Relations of Soils and Soil-Aggregate Mixtures, Using 5.5-lb (2.49 kg) Rammer and 12-in. (304.8-mm) Drop (D 698)] dry density at the dry and wet side, respectively. The compaction water content had influenced some of the engineering properties of compacted weathered Bangkok clay. The permeability of the specimens compacted at wet side of optimum had a coefficient of permeability two to three times less than the specimens compacted at dry side of optimum. This is believed to be due to the different structure of the fabric. The samples compacted at the dry side of optimum tend to form a

flocculated structure, while the samples compacted at the wet side tend to form a dispersed structure (Haque 1977). As in the case of direct shear test, the specimens compacted at the dry side of optimum had higher strength parameters compared to those compacted at the wet side of optimum (Hardiyatimo 1990).

Theoretical Considerations

As in conventional reinforced earth structures, the internal stability of the welded steel geogrid reinforced system consists of two basic components. The first component is the tension failure of the reinforcement, and the second is the pullout failure of the reinforcement. The former component can easily be verified for adequacy on the basis of the actual lateral stress imposed on the reinforcement of known cross-sectional area and allowable tensile stress. For the latter component, however, the mechanism of failure has not yet been fully understood and is subject to considerable research. This is especially true for the case of the welded steel geogrid reinforcement where there are two components contributing to the pullout resistance compared to a single component at the strips used in conventional earth reinforcement. The first component of the pullout resistance is that of friction between the longitudinal member of grid reinforcement and the backfill material, which is basically the only source of resistance for strip reinforcement. This frictional component of the pullout resistance is quite easily understood and determined theoretically. The second component of the pullout resistance is the bearing resistance offered by the transverse member. Unlike the first, the mechanism responsible for providing pullout resistance to the transverse member is not well understood and has been determined only empirically from laboratory pullout tests (Bishop and Anderson 1979; Peterson and Anderson 1980; Nielsen and Anderson 1984).

The total pullout resistance of the reinforcement (F_t) can be expressed as follows

$$F_t = F_f + F_b \quad (1)$$

The frictional resistance (F_f) developed along the longitudinal members of the reinforcement is taken as (Peterson and Anderson 1980)

$$F_f = A_s \sigma'_v \tan \phi \quad (2)$$

where A_s is the frictional area of the reinforcement, σ'_v is the average normal stress usually taken as $0.75\sigma_v$ in which σ_v is the vertical overburden pressure and ϕ is the friction angle between reinforcement and soil. The passive or bearing resistance (F_b) of the transverse members is related to the cohesion, friction angle and the bearing capacity factors in the Terzaghi-Buisman bearing-capacity equation, which was modified in the following form (Peterson and Anderson 1980)

$$F_b/(nwd) = cN_c + \sigma_v N_q \quad (3)$$

where

n = the number of transverse members,

w = the width of the reinforcement, and

N_c and N_q = the bearing capacity factors.

The expression for N_q depends on the assumed failure mechanism such as bearing failure mode (Peterson and Anderson 1980) or punching failure mode (Jewell et al. 1984) as illustrated in Fig. 2. The value for N_c is taken as $\cot \phi (N_q - 1)$. A study by Ospina (1988) based on X-ray monitored pullout tests conducted on wire mesh embedded in sand indicated that the failure mechanism was a function of the allowed deformation of the wire mesh and the normal confining pressure. It was observed that the mechanism of failure in front of a transverse member embedded in loose sand is a bearing capacity failure. At the dense state, a punching failure seemed to develop in front of the transverse members at low deformations, which became a bearing capacity failure at larger deformations. Furthermore, at low normal confining pressures, the failure mechanism was closely related to a punching type failure while bearing capacity failure was noted for high normal confining pressures.

Pullout Tests

In the laboratory, pullout tests were conducted using a 1.30 by 0.80 by 0.50-m (50 by 30 by 20 in.) test cell made up of 13.0-mm (1/2-in.)-thick steel plates (Fig. 3). A typical test setup for the laboratory pullout test is shown in Fig. 4. The vertical stress was supplied by an air bag fitted inside the pullout box between 6.5-mm (1/4-in.) flexible metal plates. The pullout force, measured by means of an electronic load cell, was applied to the test specimen using an electrically controlled hydraulic cylinder mounted against the supporting frame of the pullout cell. The horizontal displacement of the mat was monitored using the linear variable differential transformer (LVDT) and was pulled out at a rate of 1 mm/min. The data acquisition system (21 × micrologger) recorded both the mat displacement, pullout force, and the axial strains in the longitudinal and transverse members by means of strain gages. The reinforcements consisted of 6.5-mm (1/4-in.), 9.5-mm (3/8-in.), and 13.0-mm (1/2-in.)-diameter bars with various mesh sizes of 0.15 by 0.23-m (6 by 9-in.), 0.15 by 0.30-m (6 by 12-in.), and 0.15 by 0.35-m (6 by 18-in.). The weathered clay backfill materials were compacted at 95% standard Proctor (ASTM D 698) densities at dry side and wet side of optimum water contents. A typical schematic diagram of the welded steel geogrid reinforcement used in laboratory tests is shown in Fig. 5.

A full-scale, mechanically stabilized wall/embankment system with welded steel geogrid reinforcements (Fig. 6) was constructed inside the Asian Institute of Technology campus, located 42 km north of Bangkok. It has a vertical wire-mesh facing on one side and a sloping back. It consists of three sections with three different backfill materials, namely, weathered clay, clayey sand, and lateritic residual soil. The backfill materials were compacted at 95% standard Proctor (ASTM D 698) densities with placement water content varying by about $\pm 1\%$ corresponding to that density, generally on the dry side of optimum. Dummy reinforcement specimens were installed during the construction of the embankment at different levels in the vertical wall for field pullout tests. Field pullout tests were conducted to investigate the pullout resistance of reinforcements embedded at representative overburden, field moisture, and density conditions. There were five dummy reinforcement specimens embedded in the weathered clay section (see Fig. 6a). The details of the dummy reinforcement are given in Fig. 7. The dummy reinforcements were pulled out using the same strain rate (1 mm/min) and test procedure as adopted in the laboratory pullout test. The pullout

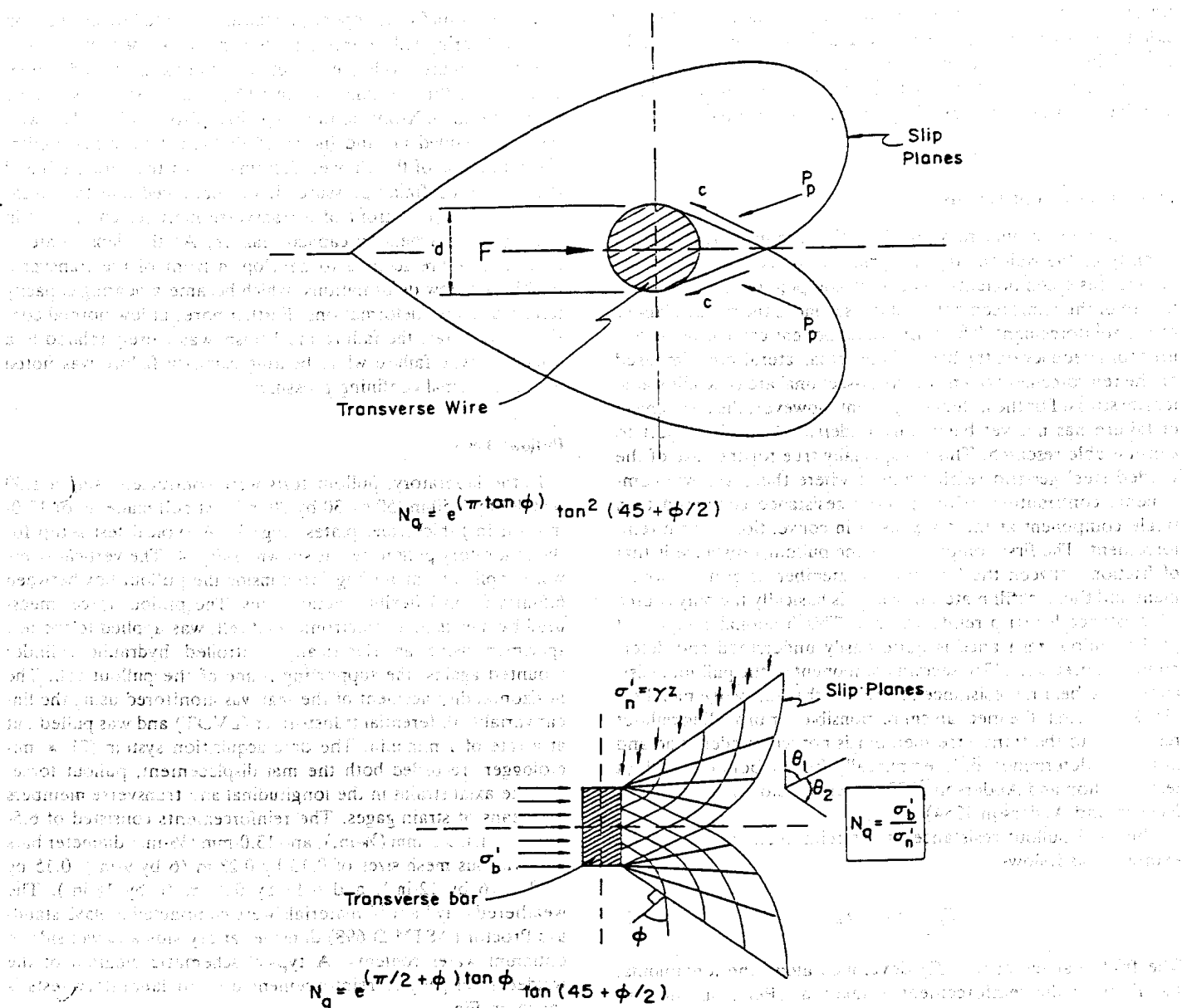


FIG. 2—Failure mechanisms with respective expressions for N_q : (top) bearing capacity failure (after Peterson and Anderson, 1980) (bottom) punching shear failure (after Jewell et al. 1984).

force was applied similar to that in the laboratory with a specially designed reaction frame butting against the wall face of the mechanically stabilized wall-embankment system. A wooden platform was built to support the pullout equipment when testing for dummy reinforcements located at higher levels in the wall. A typical test setup for field pullout test is shown in Fig. 8.

Results and Analyses

Typical stress-strain relationships from laboratory pullout tests are shown in Figs. 9 and 10, for dry and wet side compactions, respectively. The typical stress-strain relationships from field pullout tests are shown in Fig. 11. In the laboratory, it was observed that the pullout resistance with backfill materials compacted at wet side of optimum was lower compared to that of the dry side of optimum. This was attributed to the higher strength

of soil compacted at the dry side of optimum than that at the wet side of optimum. Generally, the pullout resistance increased with increasing applied normal pressure as in the case of high-quality backfill materials. The plots of strain with distance from the facing are typically shown in Figs. 12 and 13 for dry and wet side compactions, respectively. The results indicate linear variation of strains in the order of 0.01 to 0.20% only. This means a maximum of 2-mm elongation for a 1.0-m longitudinal bar which is very small compared to about 25-mm pullout displacement. It is therefore reasonable to consider that the reinforcement moved nearly as a rigid body and that the pullout resistance along the reinforcement is uniformly mobilized. The levels of strains were also found to reduce when the backfill compaction varied from dry side to wet side of optimum, with the dry side exhibiting a steeper slope of strain variation with distance. This implied that at the dry side compaction, in which the soil was

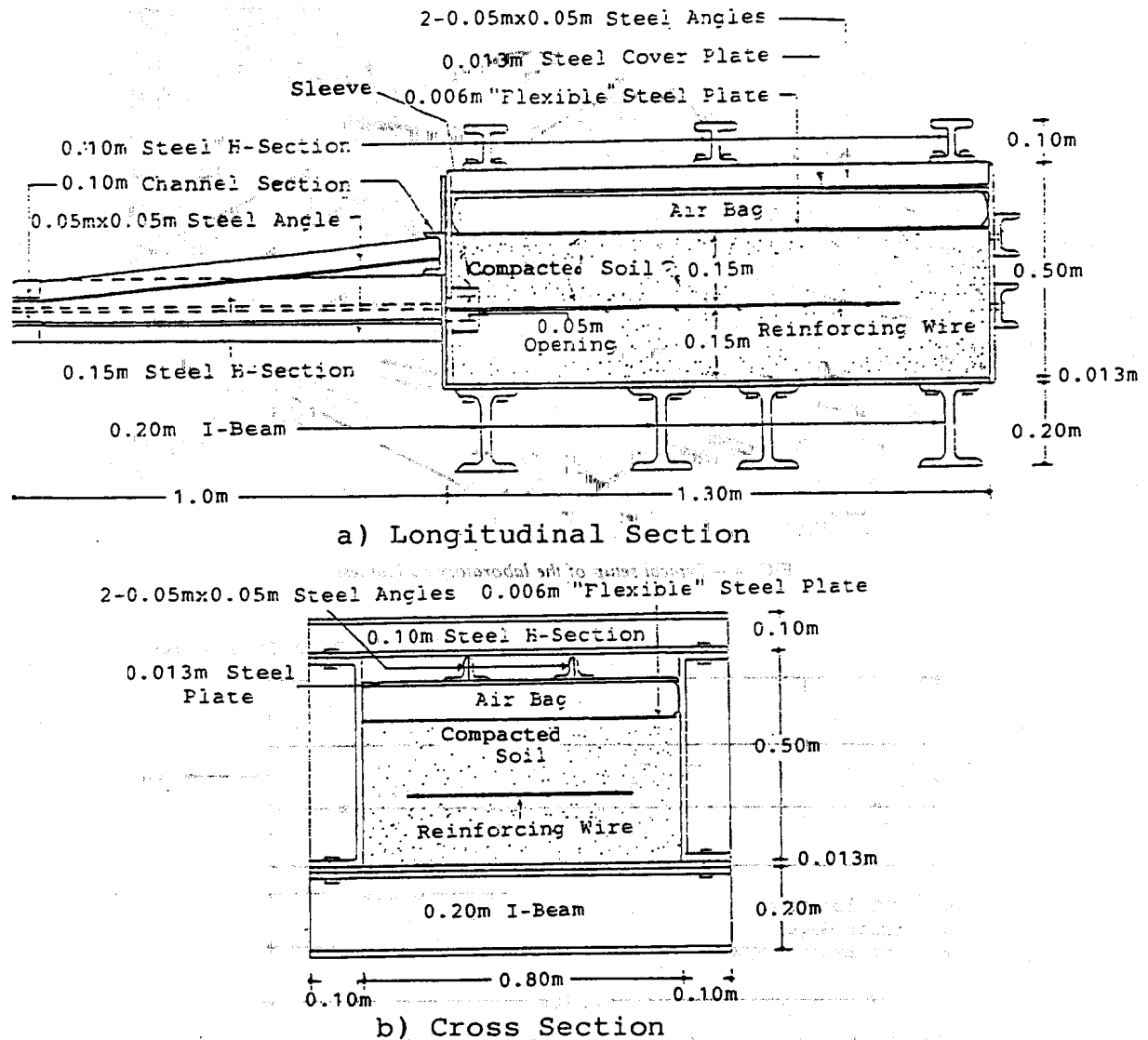


FIG. 3—Schematic diagram of the laboratory pullout testing cell.

the relative movement of the reinforcement with respect to the backfill soil was smaller compared to that of the wet side, causing higher induced strains in the reinforcement (Bergado et al. 1990). The maximum pullout resistances for different mesh sizes seemed to indicate that the 0.15 by 0.23-m (6 by 9-in.) mesh size was superior for both the dry and wet compacted backfill materials. Reinforcements with their transverse members removed were tested to determine the contribution of the longitudinal members through adhesion/friction to the backfill material. As expected for poor quality backfills, the ad component was quite minimal at about 5 to 15% of the pullout resistance. Figure 14 shows the relationship between the passive bearing resistance per unit area, F_p/nwd , and applied normal pressure for the two bar diameters, namely, 6.5 mm ($\frac{1}{4}$ -in.) and 13.0 mm ($\frac{1}{2}$ -in.). The notation F_p stands for pullout bearing force, n is the number of transverse members, w is the width of the reinforcement specimen, and d is the diameter of transverse members. In the case of 6.5-mm ($\frac{1}{4}$ -in.)-diameter reinforcements, lower normal pressures were applied compared to that of 13.0-mm ($\frac{1}{2}$ -in.)-diameter reinforcements because ten-

sion failures occurred in 6.5-mm ($\frac{1}{4}$ -in.) reinforcement at higher normal pressures. It was generally observed that the 6.5-mm ($\frac{1}{4}$ -in.)-diameter reinforcements yielded higher F_p/nwd values than that of 13.0-mm ($\frac{1}{2}$ -in.) diameter. This may be attributed to the fact that the passive bearing resistance for smaller diameter bars is fully mobilized. A similar study (Palmiera and Milligan 1989) supporting this observation indicated that a larger S/D ratio resulted in higher pullout bearing resistance up to a certain limit, where S is the spacing between transverse members and D is the diameter of the transverse member.

Comparing the stress-strain relationships from laboratory pullout tests (Figs. 9 and 10) with that from field pullout tests (Fig. 11), it was observed that laboratory tests yielded a peak pullout resistance at relatively low displacement, while the peak pullout resistance from the field tests occurred at higher displacement. This suggests that the elongation for longer reinforcement resulted in more displacement to reach the yield load for the same overburden pressure. The comparison between laboratory and field pullout resistances was made by plotting the maximum pullout resistances against normal pressures as shown in Fig. 15. It

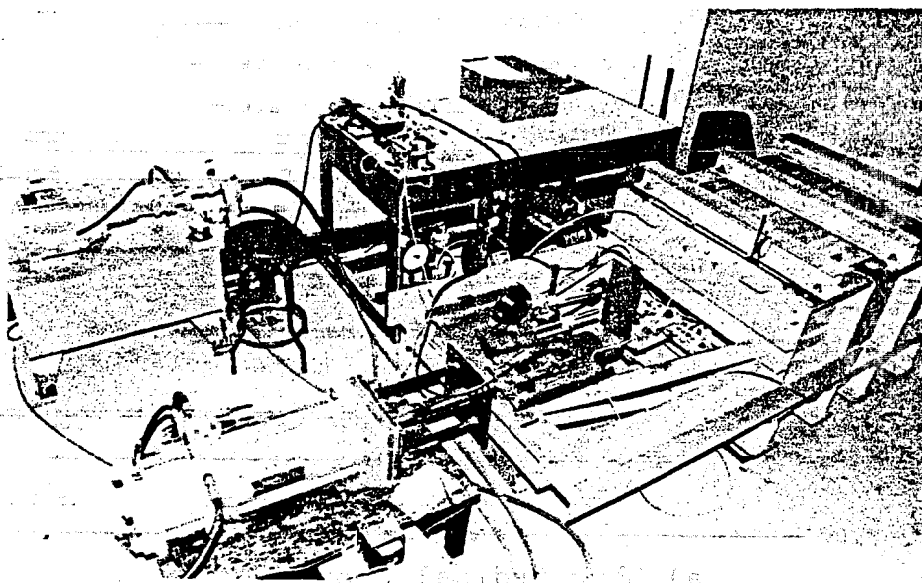


FIG. 4—Typical setup of the laboratory pullout test.

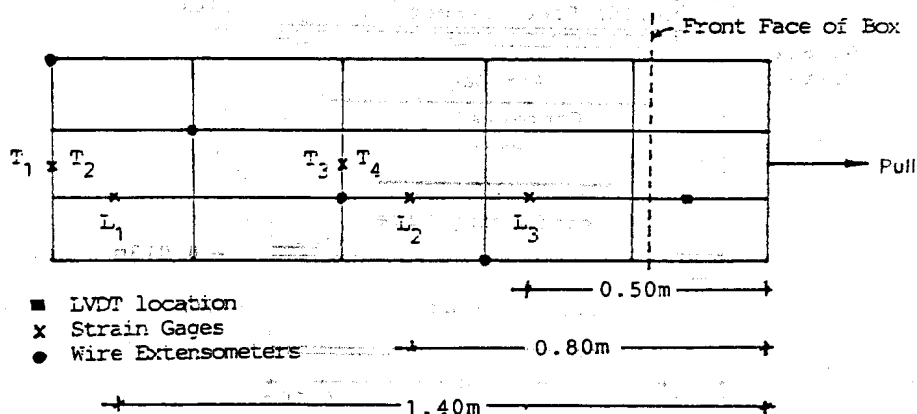


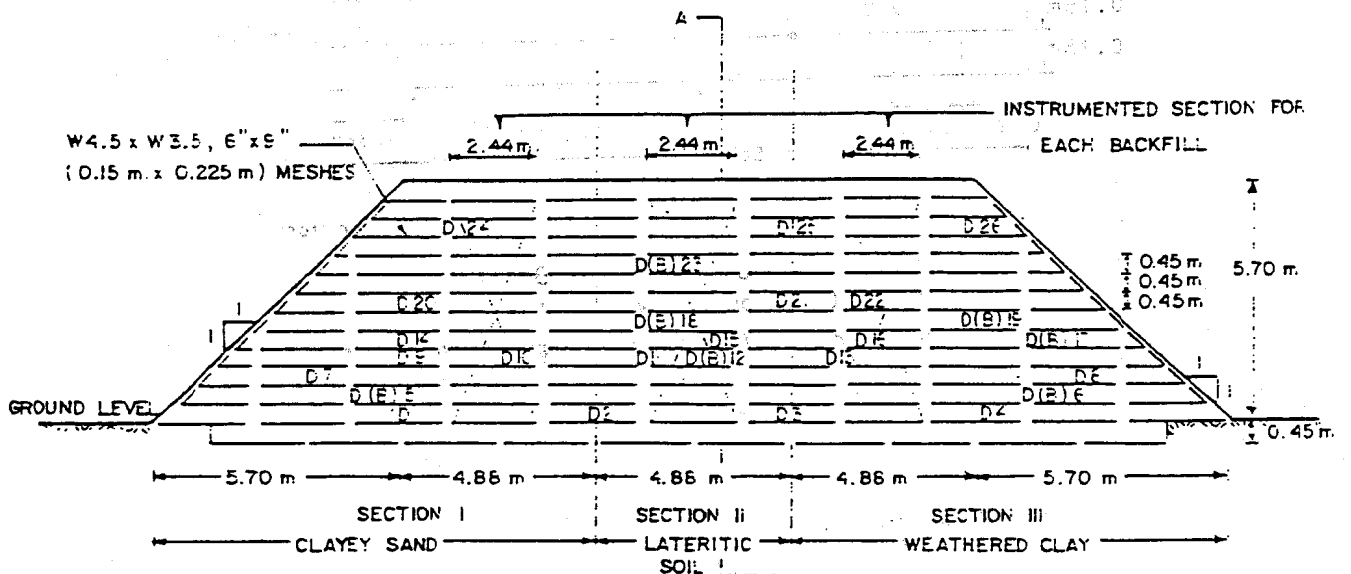
FIG. 5—Typical schematic diagram of the steel geogrid reinforcement used in the laboratory pullout test.

can be seen that the field tests provided higher pullout resistance than that of laboratory tests. One of the reasons may be due to the longer embedment length employed in the field tests. Longer reinforcements were observed to have higher peak pullout resistance for the same overburden pressure (Chang et al. 1977). The other reasons could be due to the variations in sample compaction, boundary effects in pullout apparatus, scale effect, and arching effect in the embankment system. The interaction between soil-reinforcement system and the rigid boundaries of the pullout box (especially the front face) in small-scale tests can affect the measured pullout resistance. As the reinforcement was pulled out from the box, lateral pressures could have also developed against the rigid front face, leading to the arching of the soil over the reinforcement near the front face, which reduces the local vertical stress on the reinforcement, and consequently, a decrease in the pullout resistance (Palmiera and Milligan 1989; Juran et al. 1988). The arching effects in the embankment system near the face of the wall resulted from the relatively higher settlement in the middle section (lateritic residual soil section) of the embankment. The vertical stress (overburden) at the mid-

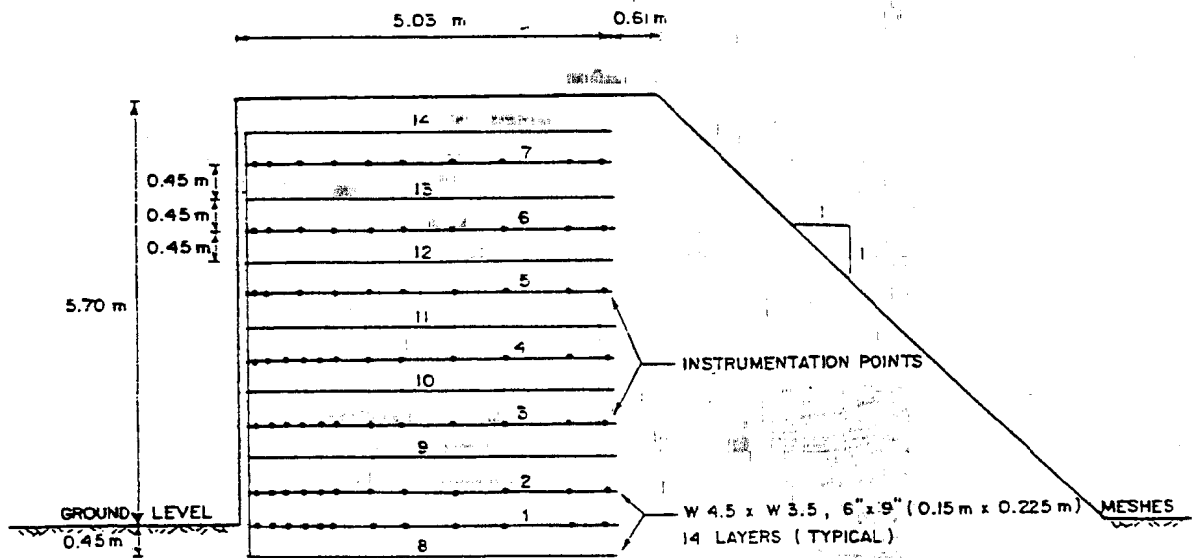
dle section, which suffered higher settlement, could be distributed to the end sections (i.e., weathered clay and clayey sand sections), which have lower settlement (Fig. 16). The distribution of vertical stress from the middle section to both end sections of the embankment was transmitted by the interconnection in the reinforcements at the face of the wall. The subsequent increase in vertical stress at the end sections provided higher pullout resistance as compared in the laboratory.

Prediction of Pullout Resistance

Figures 17 and 18 show the comparison between the predicted and observed pullout resistances. It can be seen that the prediction based on the bearing failure model (Peterson and Anderson 1980) provided an upper boundary. The prediction associated with the punching failure model (Jewell et al. 1984) offered a lower boundary. At wet side compaction, it was observed that the prediction based on the bearing failure model was closer to the observed pullout resistance than that based on the punching



D() - dummy pullout specimen



NOTE : MAT NOS. 1 TO 7 ARE INSTRUMENTED
MAT NOS. 8 TO 14 ARE NOT INSTRUMENTED

Section A-A

FIG. 6—Front and section views of the mechanically stabilized wallembankment system.

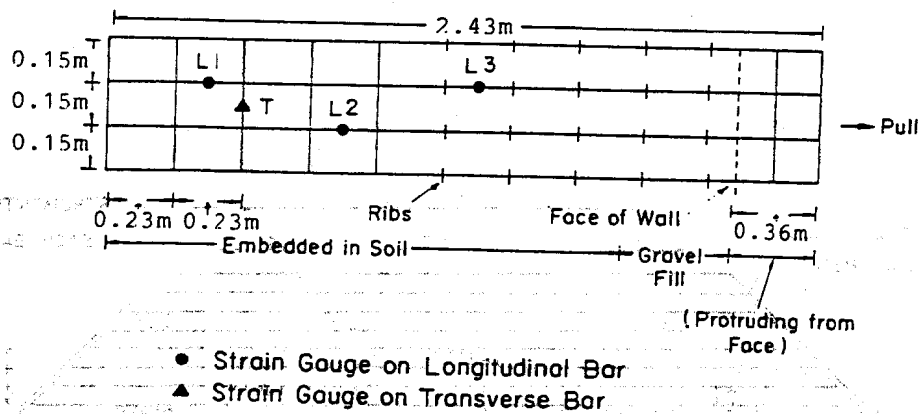


FIG. 7—Typical schematic diagram of the dummy steel geogrid reinforcement used in the field pullout test.

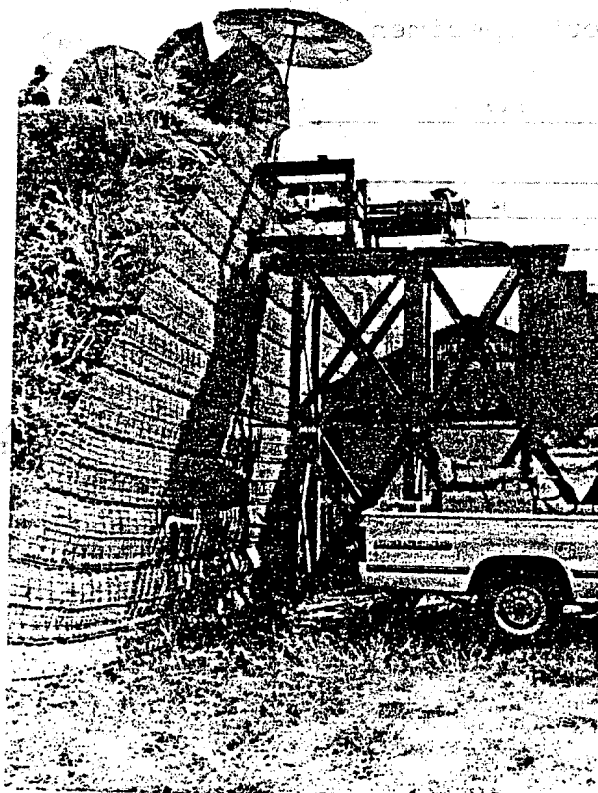


FIG. 8—Typical setup of the field pullout test.

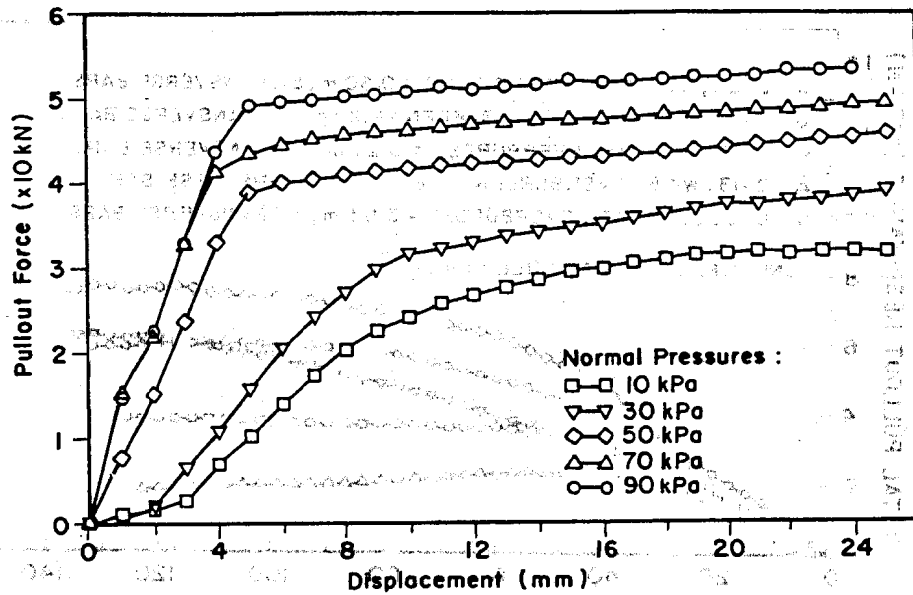


FIG. 9—Typical load-displacement curves from laboratory pullout tests for a 6.5-mm-diameter bar with 150 by 230-mm mesh size (dry side compaction).

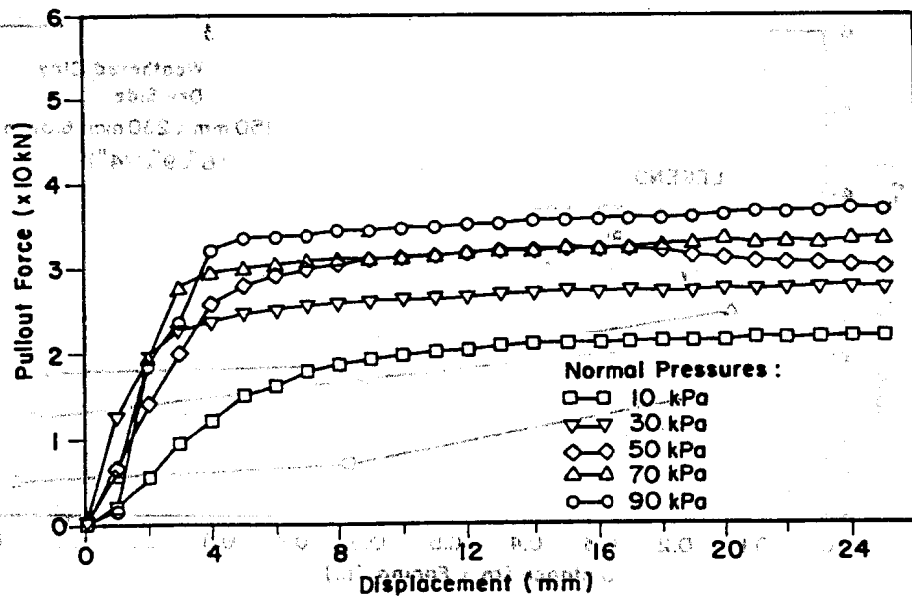


FIG. 10—Typical load-displacement curves from laboratory pullout tests for 6.5-mm-diameter bar with 150 by 230-mm mesh size (wet side compaction).

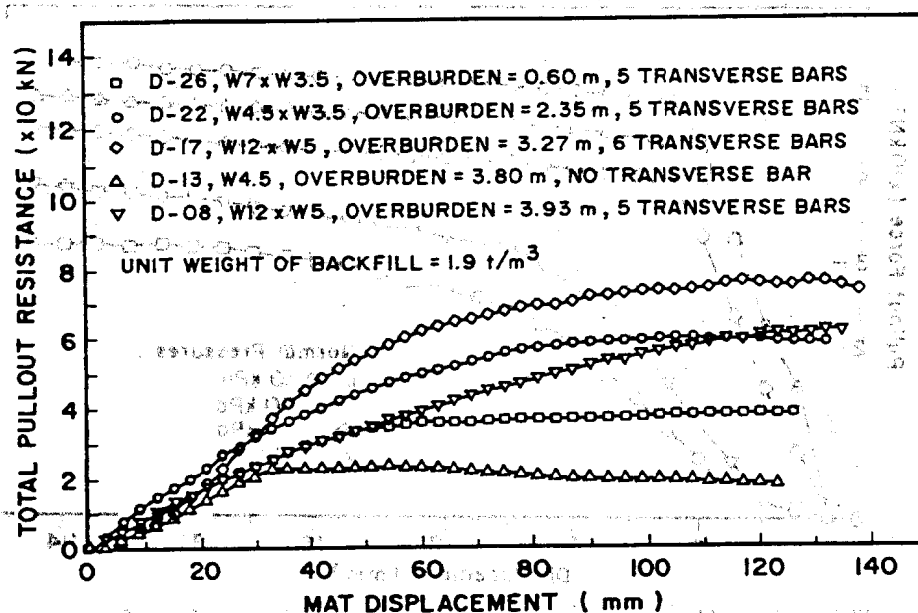


FIG. 11—Typical load-displacement curves from field pullout tests.

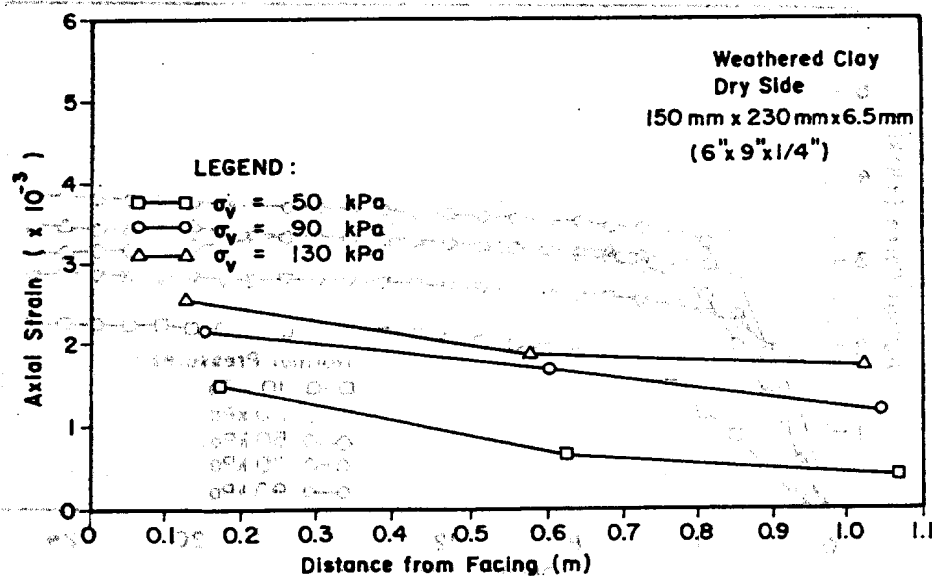


FIG. 12—Variation of axial strain with distance from facing (dry side compaction).

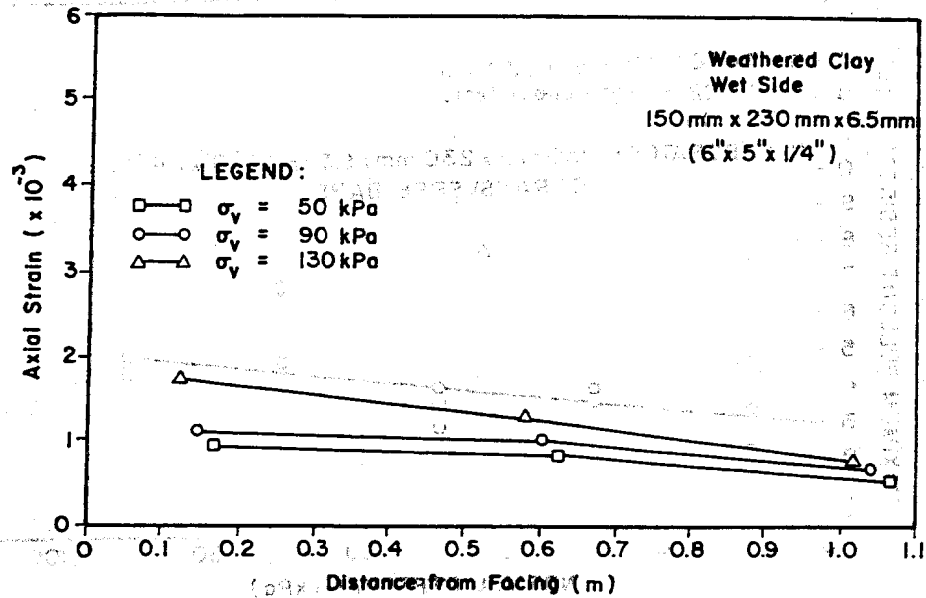


FIG. 13—Variation of axial strain with distance from facing (wet side compaction).

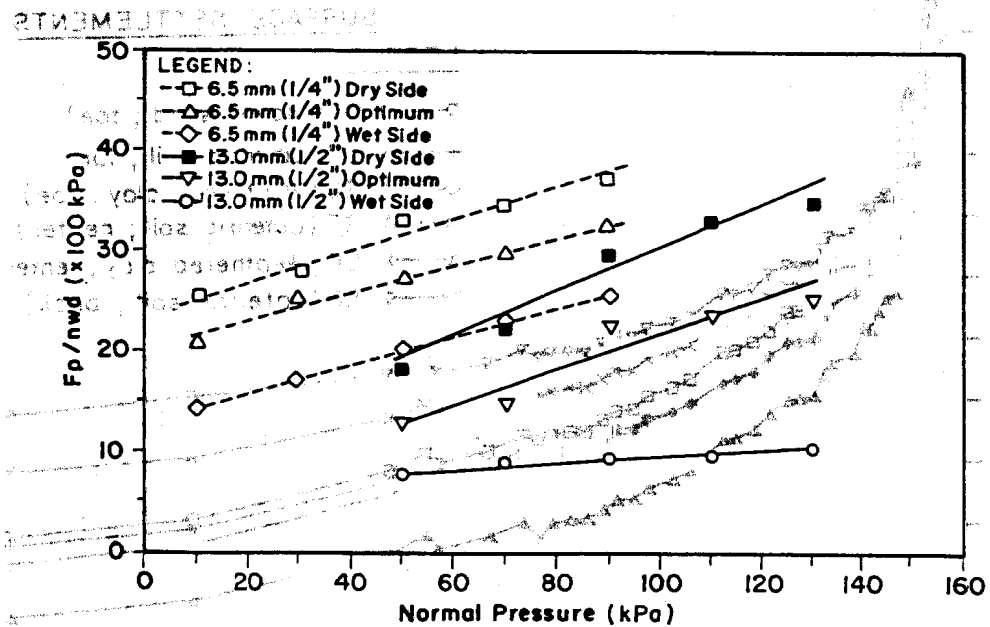


FIG. 14—Comparison of pullout resistance for different sizes of transverse bars.

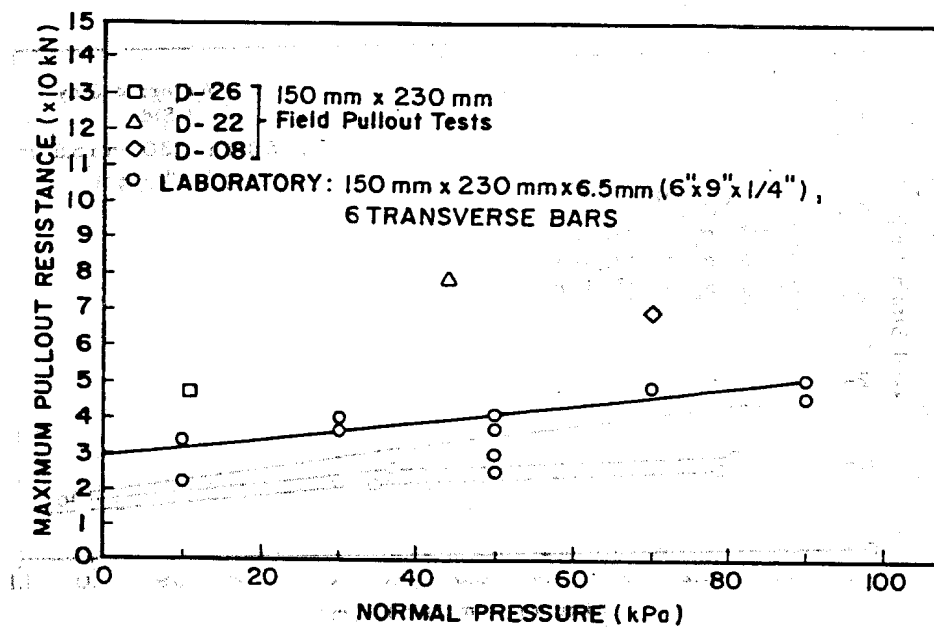


FIG. 15—Comparison of maximum pullout resistance from laboratory and field pullout tests.

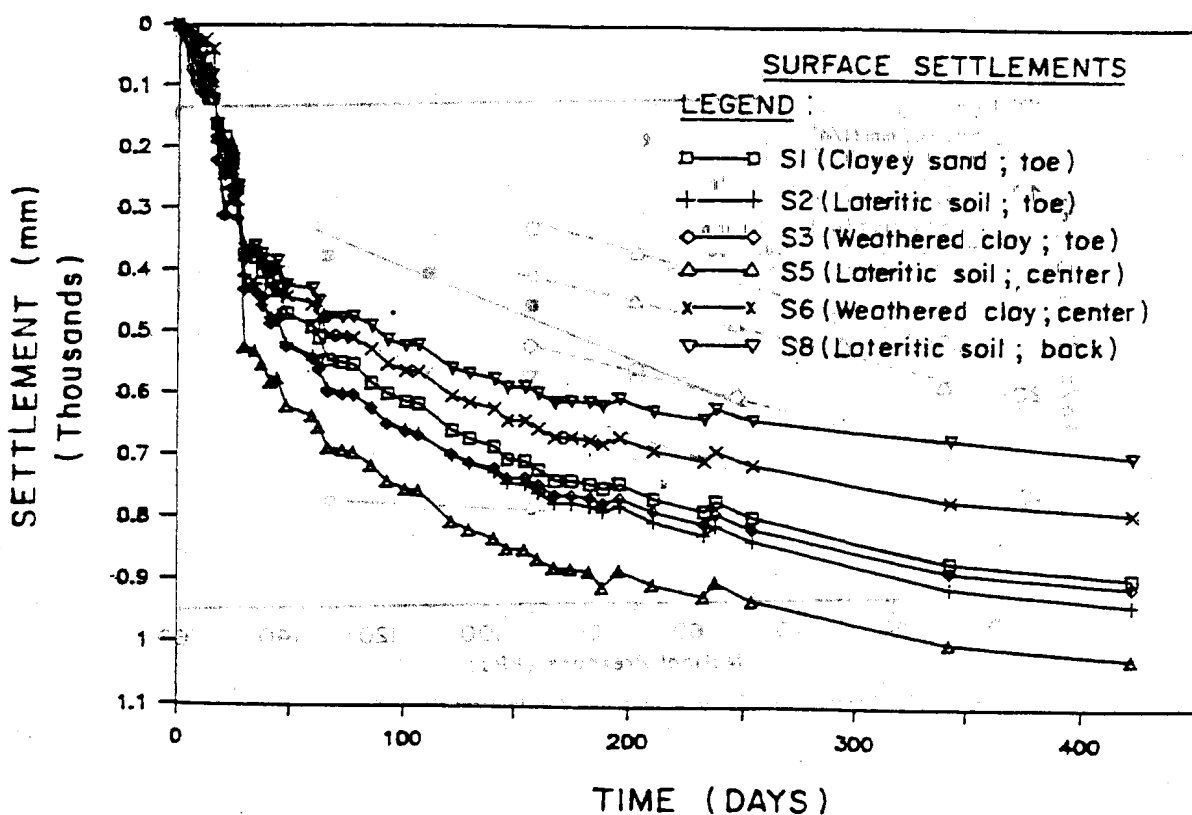


FIG. 16—Observed surface settlements beneath the mechanically stabilized wall/embankment system.

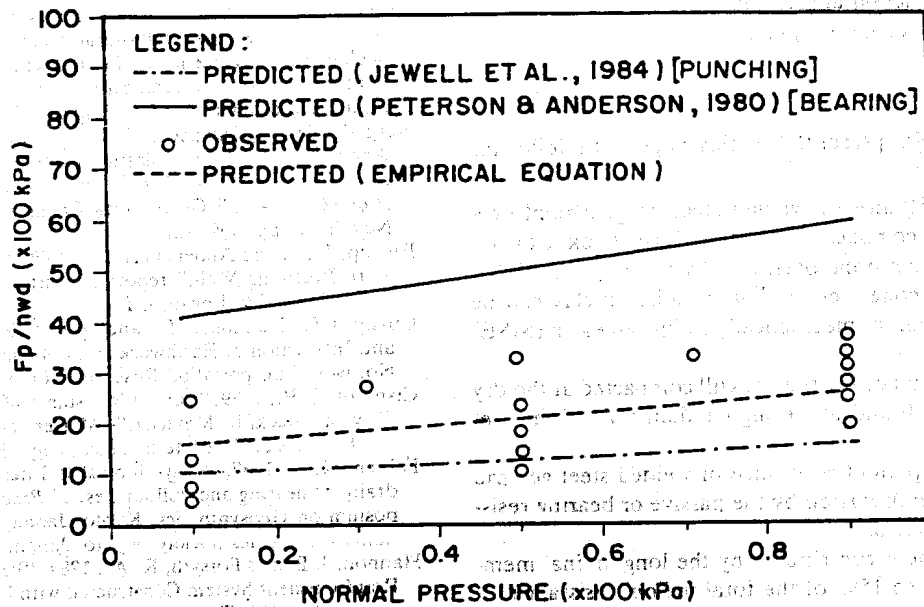


FIG. 17—Comparison of observed and predicted pullout resistance (dry side compaction).

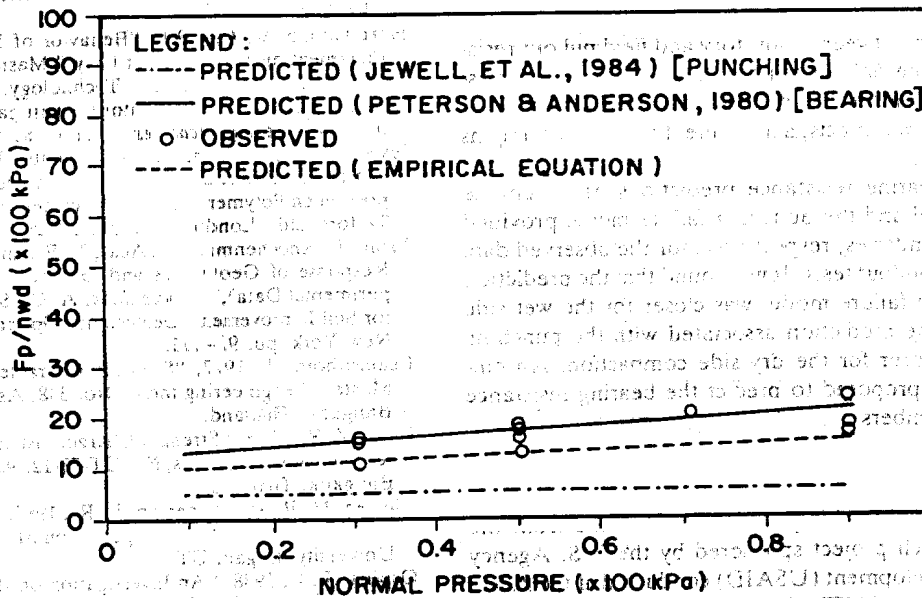


FIG. 18—Comparison of observed and predicted pullout resistance (wet side compaction).

failure model. At dry side compaction, the prediction associated with the punching failure model was closer to the observed data. It was indicated in the previous section that, at dry side compaction, relative displacement between the reinforcement with respect to the backfill soil was smaller compared to the wet side. Therefore, for large relative displacements, the failure mechanism seemed to conform with the bearing failure model. For small relative displacements, the failure mechanism was in conformity with the punching failure model.

An empirical equation for the bearing resistance (F_b) is proposed based on test data which takes the form

$$F_b = A_b N_c C_u \quad (4)$$

where

A_b = the bearing area,

N_c = an empirical number equal to 13 for weathered Bangkok clay, and

C_u = the apparent undrained strength of the backfill defined as (Ingold 1983)

$$C_u = C + \sigma_v \tan \phi \quad (5)$$

where

C = the cohesion intercept

ϕ = the internal friction angle, and
 σ_v = the vertical overburden pressure.

Conclusions

Based on test results presented in this paper, the following conclusions can be drawn:

1. The pullout resistance of welded steel geogrid reinforcements embedded in compacted weathered Bangkok clay increased with increasing normal pressure. This demonstrated that the locally available, cohesive-frictional weathered clay can be used as backfill material for mechanically stabilized earth (MSE) constructions.

2. The pullout resistance for the backfill compacted at the dry side of optimum was found to be higher than that of the wet side.

3. The bulk of the pullout resistance of welded steel geogrid reinforcements was being carried by the passive or bearing resistance mobilized in front of the transverse members. The adhesion/frictional component contributed by the longitudinal members was only about 5 to 15% of the total pullout resistance.

4. The maximum strain in the longitudinal members at the reinforcement amounted to about 0.01 to 0.20%, indicating that the reinforcement moved nearly as a rigid body and that the pullout resistance along the reinforcement was uniformly mobilized.

5. The comparison between laboratory and field pullout resistance revealed that the field tests provided higher pullout resistance due to the influences of compaction density and water content, arching and scale effects, and different embedment lengths of pullout specimens.

6. The pullout bearing resistance predictions based on the bearing failure model and the punching failure model provided upper and lower boundaries, respectively, for the observed data from the laboratory pullout tests. It was found that the prediction based on the bearing failure model was closer for the wet side compaction, while the prediction associated with the punching failure model was closer for the dry side compaction. An empirical equation was proposed to predict the bearing resistance of the transverse members with reasonable accuracy.

Acknowledgments

The results presented in this paper were obtained from the execution of a research project sponsored by the U.S. Agency for International Development (USAID) conducted at the Asian Institute of Technology (AIT), Bangkok, Thailand with joint cooperation from Utah State University, Logan, Utah. The financial assistance given by USAID, Bangkok, Thailand, and the facilities provided by the AIT are gratefully acknowledged.

References

- Abdel-Motaleb, A. A., 1989, "Pullout Resistance of Welded Wire Mats Embedded in Clayey Silt Backfill," master's thesis, Utah State University, Logan, UT.
- Bergado, D. T., Sampaco, C. L., Shivashankar, R., Alfaro, M., Anderson, L. R., and Balasubramaniam, A. S., 1990, "Interaction of Welded Reinforcement with Poor Quality Backfill," *Proceedings, Southeast Asian Geotechnical Conference*, Taipei, Vol. 1, South Asian Geotechnical Society, Taipei, Taiwan, pp. 29-34.
- Bergado, D. T., Sampaco, C. L., Shivashankar, R., Alfaro, M., Anderson, L. R., and Balasubramaniam, A. S., 1991, "Performance of a Welded Wire Wall with Poor Quality Backfills on Soft Clay," *Proceedings, ASCE Geotechnical Congress*, Boulder, Colorado, ASCE, New York, pp. 909-922.
- Bishop, J. A., and Anderson, L. R., 1979, "Performance of the Wire Retaining Wall," report submitted to Hilfiker Pipe Co., Utah State University, Logan, UT.
- Chang, J. C., Hannon, J. B., and Forsyth, R. A., 1977, "Pull Resistance and Interaction of Earthwork Reinforcement and Soil," TRB Report No. 640, Transportation Research Board, Washington, DC.
- Cisneros, C. B., 1989, "Pullout Resistance of Steel Grids with Weathered Clay as Backfill Material," Master of Engineering thesis, GT-88-7, Asian Institute of Technology, Bangkok, Thailand.
- Fabian, K. J., 1987, "Clay-Geotextile Interaction in Drained and Undrained Shearing and Pullout Tests," *Proceedings, International Symposium on Geosynthetics*, Kyoto, Japan, Japan Chapter of International Geotextiles Society, Kyoto, Japan, pp. 93-102.
- Hannon, J. B. and Forsyth, R. A., 1984, "Performance of an Earthwork Reinforcement System Constructed with Low Quality Backfill," Report No. 965, Transportation Research Board, National Research Council, Washington, DC.
- Haque, M. A., 1977, "Some Engineering Properties of Compacted Red Clay Evaluated on the Basis of Laboratory Tests," Master of Engineering thesis, No. 1005, Asian Institute of Technology, Bangkok, Thailand.
- Hardiyatimo, H. C., 1990, "Behavior of Mechanically Stabilized Earth Bankment on Soft Bangkok Clay," Master of Engineering thesis, GT-89-9, Asian Institute of Technology, Bangkok, Thailand.
- Ingold, T. S., 1983, "Laboratory Investigation of Grid Reinforcement in Clay," *Geotechnical Testing Journal*, Vol. 6, No. 3, pp. 112-118.
- Jewell, R. A., Milligan, G. W. E., Sarsby, R. W., and Dubois, D., 1981, "Interaction Between Soil and Reinforcement," *Proceedings, Symposium on Polymer Grid Reinforcement in Civil Engineering*, Thomas Telford Ltd., London, UK, pp. 19-29.
- Juran, I., Knochenmus, G., Acar, Y. B., and Arman, A., 1988, "Pull Response of Geotextiles and Geogrids (Synthesis of Available Experimental Data)," *Proceedings, ASCE Symposium on Geosynthetic for Soil Improvement*, Geotechnical Special Publication No. 18, ASCE, New York, pp. 92-111.
- Leelasithorn, T., 1977, "Strength Characteristics of Compacted Clay," Master of Engineering thesis, No. 338, Asian Institute of Technology, Bangkok, Thailand.
- Liew, Y. Y., 1978, "Strength Characteristics of Compacted Clay," Master of Engineering thesis, No. GT-78-12, Asian Institute of Technology, Bangkok, Thailand.
- Nielsen, M. R. and Anderson, L. R., 1984, "Pullout Resistance of Wire Mats Embedded in Soil," report submitted to Hilfiker Co., Utah State University, Logan, UT.
- Ospina, R. I., 1988, "An Investigation on the Fundamental Interaction Mechanism of Non-Extensible Reinforcement Embedded in Sand," Master of Science thesis, Georgia Institute of Technology, Atlanta, GA.
- Palmiera, E. M. and Milligan, G. W. E., 1989, "Scale and Other Factors Affecting the Results of Pullout Tests of Grids Buried in Sand," *Geotechnique*, Vol. 39, No. 3, pp. 551-524.
- Peterson, L. M. and Anderson, L. R., 1980, "Pullout Resistance of Welded Wire Mats Embedded in Soil," Master of Science thesis, Utah State University, Logan, UT.
- Plangpongpon, S., 1977, "Strength Characteristics of Bangkok Clay Relation to Pavement Design," Master of Engineering thesis, No. 1014, Asian Institute of Technology, Bangkok, Thailand.